Physical Modelling of Non-Invasive Silicon Temperature Measurement by Infrared Absorption

J.C. Sturm and C.M. Reaves*
Department of Electrical Engineering
Princeton University, Princeton, NJ 08544

*Present address: Department of Electrical Engineering,
University California at Santa Barbara, Santa Barbara, CA

Abstract

It has recently been shown that the temperature of silicon wafers can be measured in situ in rapid thermal processing reactors by monitoring the infrared absorption of the substrate at specific wavelengths. In this paper a physical model model of infrared absorption in silicon is used to determine the dominant absorption mechanisms in the relevant temperature and wavelength ranges. The model is then used to predict the ultimate temperature ranges of applicability of the technique and to show the effects of heavy doping.

Introduction

The measurement of the silicon wafer temperature has long been a critical issue in the rapid thermal processing field. Pyrometry is unreliable because of the variation of emissivity with field oxides, wafer backside polish, doping, chamber design, wavelength, and temperature itself [1]. Errors of 100 °C are easily possible [2]. Thermocouples are also not desirable because of the reliability of the thermal contact and because of contamination concerns. The optical absorption of silicon in the infrared range is a very strong function of temperature. Using this principle, it has recently been shown that the silicon wafer temperature in an RTP reactor can be non-invasively measured from 500 to 800 °C by the in-situ observation of the transmission of light through the wafer at 1.3 and 1.55 μm (Fig.'s 1, 2) [3,4]. The low power densities of less than 1mW/cm^2 make this a non-invasive technique. While the method has an accuracy of $\sim$ 1 °C, does not require knowledge of emissivity, and has been used for the RTP-CVD epitaxial growth of Si and $Si_{1-x}Ge_x$ alloys, the basic absorption processes and limits of the technique were not known. These issues are addressed in this paper through modelling of the IR absorption in silicon.

Physical Processes

The transmitted IR light which reaches the detector depends on the silicon surface reflectivity and scattering from the rough wafer backside in addition to the desired absorption dependence. The infrared reflection is only a very weak function of temperature, however [5], and hence can be removed from the data along with other constant factors (such as the backside roughness scattering) by defining a normalized transmission n(T) which is equal to the high temperature transmission divided by the room temperature transmission of the same wafer. It is easily shown that n(T) is to first order simply $e^{-\alpha_{tot}(T)\cdot d}$, where $\alpha_{tot}(T)$ is the total absorption coefficient and d is the wafer thickness. Infrared absorption in silicon can proceed by two processes: band-to-band (bandgap) absorption (referred to as α_{BG}) and by free carrier absorption (α_{FC}) (Fig. 3). As the temperature is increased, the phonon population increases and the bandgap decreases, both of which cause an increase in the indirect bandgap absorption process in silicon. Furthermore, at high temperatures the increased phonon population increases the absorption cross section for each free carrier, and the free carrier population will increase. These effects both cause the free carrier absorption to also increase with temperature.

The bandgap absorption process can be described by the model of Macfarlane [6] which was refined by Jellison [7]. The model accounts for the emission (j=1) and absorption (j=2) of both TA (i=1, θ = 212 K) and TO (i=2, θ = 670 K) phonons and incorporates the temperature-dependent phonon distribution as well as the temperature dependence of the bandgap:

$$\alpha_{BG}(h\nu,T) = \sum_{i=1}^{2} \sum_{j=1}^{2}(-1)^j \frac{\alpha_i[h\nu - E_g(T) + (-1)^j k\theta_i]}{\exp[(-1)^j\theta_i/T] - 1} \quad (1)$$

Expressions for $\alpha_i(E)$ are given in Ref. 7. For larger photon energies more states are accessible and hence the absorption across the bandgap increases sharply. To model free carrier absorption cross section at high temperatures from first principles, one needs to know the hot carrier scattering rates at these temperatures,

CH3075-9/91/0000-0895 $1.00 © 1991 IEEE

which are not known. The temperature dependence of free carrier absorption cross section in silicon at temperatures $< 100^\circ$C has been measured previously at 1.06 μm [8]. By linearly extrapolating these results to high temperature, assuming a classical λ^2 wavelength dependence, and apportioning the cross sections into electron and hole contributions, one can estimate the absorption cross section per free carrier:

$$\sigma_n(\lambda,T) = 1.01\times10^{-12} \cdot T \cdot \lambda^2 \, K^{-1} \qquad (2)$$
$$\sigma_p(\lambda,T) = 0.51\times10^{-12} \cdot T \cdot \lambda^2 \, K^{-1}$$

By calculating the number of free carriers from the doping and the intrinsic carrier concentration, the free carrier absorption $\alpha_{FC}(T)$ can be calculated. Adding α_{FC} and α_{BG} gives the total absorption $\alpha_{tot}(T)$.

Results and Implications

The agreement of the model (no adjustable parameters) and the data (Fig. 2) is excellent, implying that the extrapolation of the low-temperature free carrier absorption data to high temperatures (800 °C) is a good approximation. The comparison of α extracted from the measurements to the modelled α_{BG} and α_{FC} (Fig. 4) shows a surprising but important result. Bandgap absorption dominates the absorption at 1.3 μm, but free carrier absorption dominates at 1.55 μm. This result was confirmed by "temperature-tuning" the semiconductor levers to shift their wavelengths by about $\sim$ 10 nm (Fig. 5). At 1.3 μm, shorter wavelengths had a much higher absorption, consistent with free carrier absorption. At 1.55 μm, however, the absorption at shorter wavelengths was slightly weaker, consistent with the λ^2 dependence of free-carrier absorption. These results may be compared with the emissivity ϵ measurements of Sato [1], shown by the solid line in Fig. 6 for 470°C. Since ϵ = 1-R-T (where R and T are the reflected and transmitted signals, respectively), one can infer the transmission as a function of wavelength. The different trends for the transmission T at 1.3 and 1.55 μm are consistent with our results.

Practical application of the technique requires 5 cm^{-1} $< \alpha_{tot} <$ 150 cm^{-1} so that some dependence of the transmission on temperature is seen, but that the incident signal is not completely absorbed. In Fig. 2 the upper temperature limit at 1.55 μm is seen to be $\sim$ 850°C because of the small transmitted signal, so that for higher temperature applications a wavelength with less absorption is required. However, our model predicts a minimum in α at 1.5 μm (Fig. 7) with α_{BG} dominating and increasing at shorter wavelength and α_{FC} dominating and increasing at longer wavelength. Therefore it appears unlikely that the technique can be applied much above 850°C even with different wavelengths. For operating at lower temperatures, shorter wavelengths with higher bandgap absorption are desired (Fig. 8). In principle, the technique appears feasible even down to 77K (using 1.0 μm, e.g.), where it may be useful for plasma etching applications. Measurements of transmission in our lab at 1.06 μm and modelling show good agreement (Fig. 9).

One area of concern is the effect of heavy substrate doping, which strongly affects $\alpha_{FC}(T)$. A comparison of the model and data for various n- and p-type substrate dopings is shown in Fig. 10, with reasonably good agreement. No additional effects such as bandgap narrowing or band-filling were incorporated into the model. Little effect is seen until substrate doping levels of $\sim 10^{18}$cm^{-3} are reached, which corresponds to a cross section through the wafer of free carriers of $\sim 5\times10^{16}$cm^{-2} free carriers. Therefore it may be inferred that such heavily doped layers such as bipolar transistor buried layers, emitters, or MOS source-drains, all of which generally have integrated dopant densities of less than 10^{16}cm^{-3}, should have little effect upon the transmission vs temperature characteristics.

Conclusions

A general model for silicon infrared absorption at elevated temperatures has been developed. Since free carrier absorption dominates at wavelengths over 1.55 μm, $\sim$ 850°C may be estimated as an upper limit for the technique of silicon temperature measurement by infrared transmission. Because bandgap absorption dominates at short wavelengths, the technique may be extended temperatures as low as 77 K. Finally, while substrate doping over 10^{18}cm^{-3} has a large effect upon the transmission vs temperature characteristics, thin highly doped layers such as source-drains are not expected to do so.

Acknowledgements

The assistance of P.V. Schwartz, M. Nardin, and M. Chbat in the laboratory is appreciated. The support of SRC, NSF, and the NJ Comm. on Science and Technology is also appreciated.

1. T. Sato, Jpn. J. Appl. Phys. **6**, 339 (1967).
2. D.W. Pettibone, J.R. Suarez, and A. Gat, Proc. Symp. Mat. Res. Soc. **52**, 209 (1986).
3. J.C. Sturm, P.V. Schwartz, and P.M. Garone, Appl. Phys. Lett. **56**, 961 (1990).
4. J.C. Sturm, P.M. Garone, and P.V. Schwartz, J. Appl. Phys. **69**, 542 (1991).
5. F. Lukes, J. Phys. Chem. Solids **11**, 342 (1959).
6. G.G. Macfarlane et al., Phys. Rev. **111**, 1245 (1958).
7. G.E. Jellison and D.H. Lowndes, Appl. Phys. Lett. **41**, 594 (1982).
8. K.G. Svantesson and N.G. Nilsson, J. Phys. C**12**, 3837 (1979).

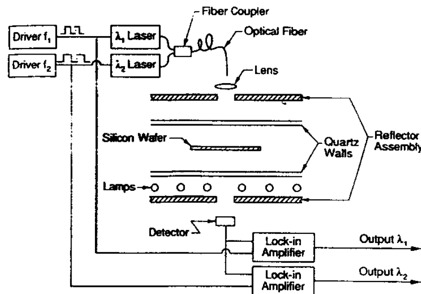

Fig. 1. Experimental reactor configuration used for measuring temperature by infrared transmission during RTCVD growth.

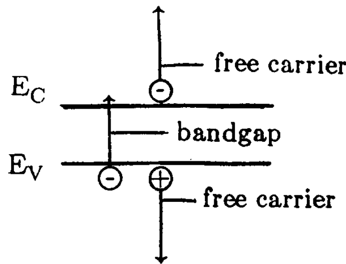

Fig. 3. Schematic illustrating bandgap (band-to-band) vs free carrier (intra-band)absorption processes.

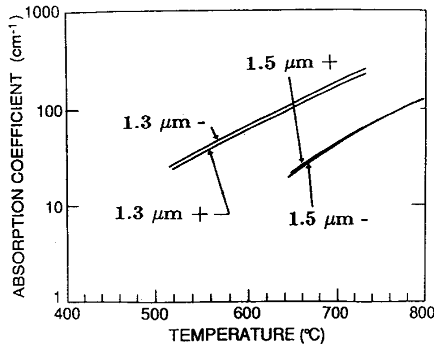

Fig. 5. Effect of temperature-tuning the semiconductor lasers on the absorption coefficient. "+" and "-" refer to slightly longer and shorter wavelengths, respectively. (This data was taken in a furnace with an uncalibrated thermocouple, so the absolute values of the data cannot be compared to those in the other figures.)

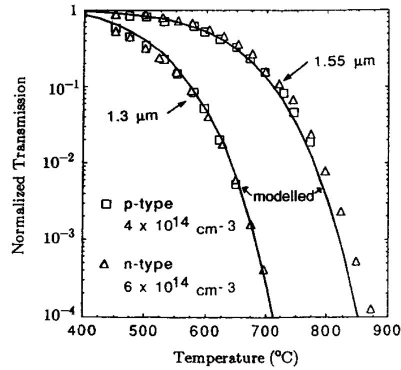

Fig. 2. Comparison of model and experimental results of normalized transmission (high temperature divided by room temperature transmission) at 1.3 and 1.55 μm.

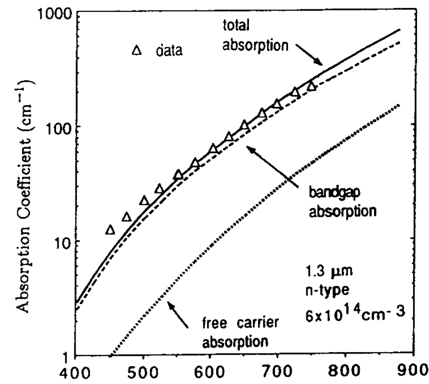

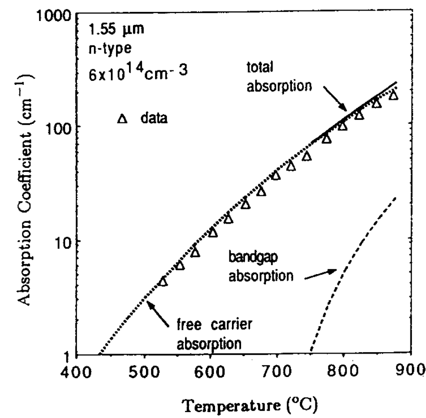

Fig. 4. Comparison of measured and modelled absorption coefficients vs temperature.

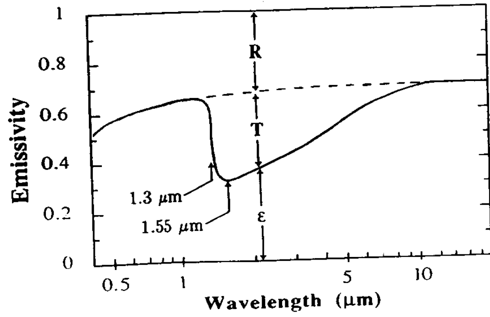

Fig. 6. Emissivity of silicon at 470 °C [1] showing a minimum near 1.5 μm, implying maximum transmission and a minimum absorption coefficient.

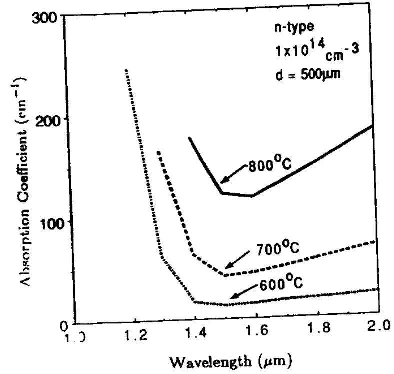

Fig. 7. Calculated absorption coefficient vs wavelength showing a minimum near 1.5 μm.

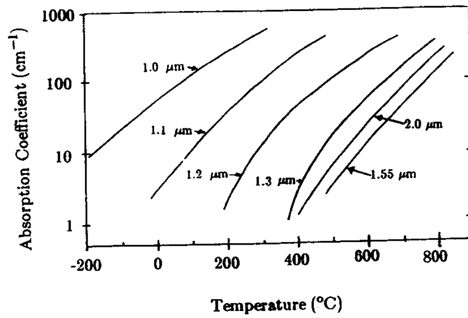

Fig. 8. Calculated absorption coefficient vs temperature at different wavelengths show the possibility of temperature measurement down to 77 K but not much above 850 °C. (α between 5 and 150 cm^{-1} required for practical application).

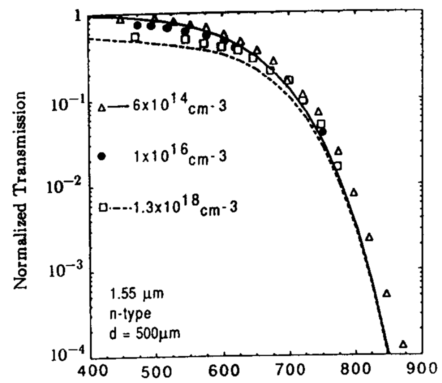

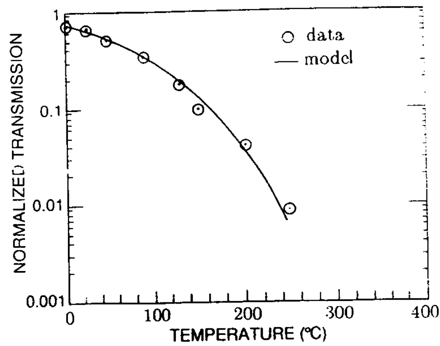

Fig. 9. Comparison of measured and modelled transmission from 0 to 250 °C at 1.06 μm.

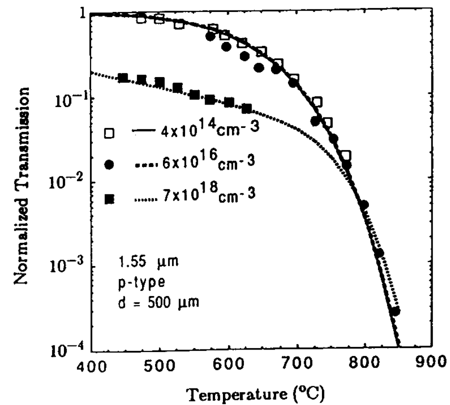

Fig. 10. Comparison of data and modelling for both (a) n-type and (b) p-type substrate doping.